J. Electrical Systems 20-3 (2024): 1741-1755

[1] B.Harika
[2] B.Suresh Kumar
[3] J.Upendar

Improvement of Voltage profile by Integrating Renewable Generation Units at weak bus locations of the System

Abstract: - The Grid consists of higher rating sources and transmission system that supports local loads. The grid operates at voltages in the range of 66kV-132kV and transmits power in MW to smaller or longer distance locations. Due to higher rating power system the power quality issues are also more. For our consideration an IEEE 14 bus interconnected system is represented as grid operating at higher rated values. The weak bus of the interconnected system is determined by Fast voltage stability index (FVSI) and load flow analysis using Newton-Raphson method available in MATLAB software. The weak buses are integrated with renewable power generation units like PV plant and wind farm improving the bus characteristics. This paper presents a comparative analysis with and without the RGUs in the system. Improvisation of the parameters like power loss, reduced conventional power consumption, power factor and voltage magnitudes are validated through time domain simulations.

Keywords: IEEE 14 bus system , FVSI, Newton-Raphson, MALTAB, Photo Voltaic (PV), Renewable generation unit (RGU)

I.INTRODUCTION

Large systems with many buses connected to multiple sources and loads have many power quality issues like voltages sags, voltage flickers, dropped power factor and high power loss etc. With longer transmission lines between the sources and loads the powers losses are increased creating voltages drops at specific bus locations. These buses are considered to be weak buses which receive low voltage levels, under compensating the loads connected to it. These power quality issues can be resolved by connecting multiple distribution generators (DGs) at the weak bus locations [1]. These DGs will compensate the local loads reducing the power consumed from the main source. The DG units connected cannot be conventional fossil fuel sources in order to mitigate global warming issue. The DG units connected at local weak buses need to be renewable sources operating in synchronization to the main grid source [2].

The renewable DG units can be solar plants, wind farms, fuel cell modules, biogas plants, tidal energy sources etc. The highest priority renewable sources are solar PV plants and wind farms because of their flexible installation locations and efficiency of the units [3]. The solar PV plants comprises of multiple PV panels arranged and connected in series parallel combinations for generation of power utilizing solar irradiation [4]. These DGs can be placed in any remote locations or even far from main grid which can be integrated to main grid by long transmission lines. However due to heavy power losses the placement of these renewable DGs must be as near possible to local bus [5].

For the analysis multiple bus system interconnected buses and many loads are considered. An IEEE 14 bus system is suitable option for the analysis, which has two main grid sources feeding 14 interconnected buses compensating multiple loads [6]. For reactive power compensation the 14 bus system is included with three static condensers at different locations [7] [8].

Figure 1 is the single line diagram of IEEE 14 bus system defining the sources, loads and condensers.

[1]Research Scholar, Dept. of Electrical Engineering, University College of Engineering, Osmania University, Hyderabad, harikagnits@gmail.com
[2] Associate Professor, Dept. of Electrical and Electronics Engineering, Chaitanya Bharathi Institute of Technology, Hyderabad
[3] Assistant Professor, Dept. of Electrical Engineering, University College of Engineering, Osmania University, Hyderabad
Copyright © JES 2024 on-line : journal.esrgroups.org

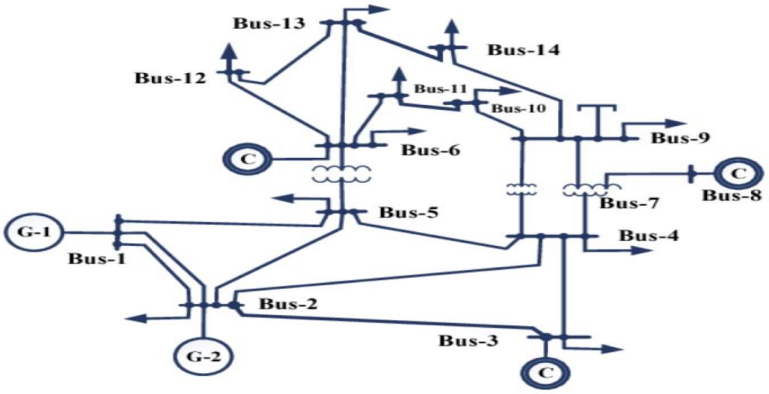

Figure 1: IEEE 14 bus single line diagram

The above bus system is analyzed using Fast voltage stability index and Newton-Raphson method of load flow analysis to determine the weak bus. The weak bus is selected depending on the FVSI value of that bus if it is approaching 1 for least loadable value. In this paper the modeling and data of IEEE 14 bus system is done in section 2 followed by configuration of DG modules for the bus system in section 3. The section 4 is included with simulation analysis of the proposed system with and without DG units connected at the weak buses. The simulation results are compared to determine the optimal bus system and the parameters are noted. The final section 5 has the conclusion to the paper which validates the generated results in the section 4.

II. SYSTEM DESIGN

To represent the system , an IEEE 14 bus grid is considered which is observed to be interconnected bus system as in figure 1 [9]. This bus system is included with two main generators G-1 and G-2 at bus 1 and 2, static condensers at buses 3, 6 and 8, loads on almost every bus respectively. The IEEE 14 bus system is designed for high rating modules in the range of 100MVA and transmission lines at 132kV. The transmission line parameters are calculated with respect to the per unit and base values considered from the below mentioned tables [10].The generators, loads, static condensers and transmission line data of IEEE14 bus system in MVA rating are given in table 1 and 2 respectively.

Table 1: Generators and load data

Bus	**GENERATION**		**LOAD**	
No.	REAL (MW)	REACTIVE (MVAR)	REAL (MW)	REACTIVE (MVAR)
1	232.4	16.9	0.0	0.0
2	40.0	42.4	21.7	12.7
3	0.0	23.4	94.2	19.0
4	0.0	0.0	47.8	3.9
5	0.0	0.0	7.6	1.6
6	0.0	17.4	11.2	7.5
7	0.0	0.0	0.0	0.0
8	0.0	12.2	0.0	0.0
9	0.0	0.0	29.5	16.6
10	0.0	0.0	9.0	5.8
11	0.0	0.0	3.5	1.8
12	0.0	0.0	6.1	1.6
13	0.0	0.0	13.5	5.8
14	0.0	0.0	14.9	5.0

Table 2: Transmission line data

Line No.	From Bus	To Bus	Line Resistance (pu)	Line Reactance (pu)
1	1	2	0.01938	0.05917
2	1	5	0.05403	0.22304
3	2	3	0.04699	0.19797
4	2	4	0.05811	0.17632
5	2	5	0.05695	0.17388
6	3	4	0.06701	0.17103
7	4	5	0.01335	0.04211
8	4	7	0	0.20912
9	4	9	0	0.55618
10	5	6	0	0.25202
11	6	11	0.09498	0.1989
12	6	12	0.12291	0.25581
13	6	13	0.06615	0.13027
14	7	8	0	0.17615
15	7	9	0	0.11001
16	9	10	0.03181	0.08450
17	9	14	0.12711	0.27038
18	10	11	0.08205	0.19207
19	12	13	0.22092	0.19988
20	13	14	0.17093	0.34802

With the above data and single line diagram given in figure 1 the IEEE 14 bus system is modeled with three phases [11]. The generators, condensers and load data are given in SI units where as the line data are represented in per units. The base values of the resistance (R) and inductance (L) for the lines are calculated by the expressions below.

Base apparent power rating of the system considered (S_{base}) = 100MVA

Base voltage rating of the system considered (V_{base}) = 132kV

$$Z_{base} = \frac{(V_{base})^2}{S_{base}} \quad (1)$$

$$= \frac{(132kV)^2}{100MVA} = 174.24\ \Omega$$

$$L_{base} = \frac{Z_{base}}{\omega} \quad (2)$$

$$= \frac{174.24}{2\pi.50} = 0.5546\ \text{H}$$

FVSI: Fast Voltage Stability Index

The FVSI index is commonly used to detect voltage collapse and contingency analysis in the power system due to line outages. This index is based on a relatively simple mathematical formula that helps to speed up the process of analyzing voltage stability. During analysis, it was observed that the line with an index near to 1.00 would be recognized the most crucial line, which refers to a bus that has the ability to make the entire system unstable. It should be considered, that at this point, it is the maximum permissible reactive load that can be connected to the bus. If the reactive load increases beyond this limit, then system collapses.

The maximum possible load can be arranged in ascending order to rank the buses of the system. The bus having least maximum permissible load is ranked first in the list, indicating that it is the weakest bus within the system.

The FVSI is prescribed as:

$$\mathbf{FVSI_{ij}} = \frac{\mathbf{4Z^2Q_j}}{\mathbf{V_i^2X}} \quad (3)$$

where, V_i is sending-end voltage for i_{th} bus, Z is impedance of the line i-j, X is reactance of the line i-j, and Q_j is reactive power at the receiving-end for j_{th} bus.

Table 3**:** Maximum load-ability limit for IEEE 14-Bus system

Bus number	Maximum Load-ability limit	FVSI Index
1,2,3,6,8	Generator bus	-
4	68	0.9937
5	67.6	0.9901
9	115	0.9915
10	111	0.9975
11	56	0.9926
12	47	0.9914
13	31	0.9769
14	32	0.9970

From table 3 it is clear that Bus 13 and Bus 14 have least maximum load-ability limits; hence, these are recognized as the weakest bus of the system respectively. Hence, this place may be assumed to be the best location for the placement of a DG.

III RENEWABLE GENERTION UNITS CONFIGURATION

As previously mentioned in section 1 from the available renewable sources the PV plant and wind farm are considered to be viable and flexible option to be installed in a grid. These two sources can be placed with a common coupling single inverter sharing combined power to the grid. However, as per the requirement of the system these two renewable sources need to be placed at different bus locations individually with individual inverters. Each renewable DG unit has its own control unit and converters which are independent on each other. The configuration of the modules used for each renewable sources are described below.

A. PV Plant

The solar PV plant is an arrangement of several PV panels in parallel and series combinations connected as per the voltage and power rating needed. The series connection of the panels increases the DC voltage amplitude of the series panel's string. Several strings are connected in parallel for increase in the current amplitude in turn increasing the power of the PV plant [12]. The PV panels are dependent source on natural solar irradiation and ambient temperature which are unpredictable. Therefore with variation of the solar irradiation and temperature the current output of the PV panel will vary linearly. In order to extract maximum power from the PV array (series and parallel combination panels represent as array) a boost converter is included which even boosts the voltage of the PV array. The output voltage of the boost converter is set by the inverter control module which will be predefined during the operation of the system [13]. The circuit topology of PV array and boost converter module can be observed in figure 2 below.

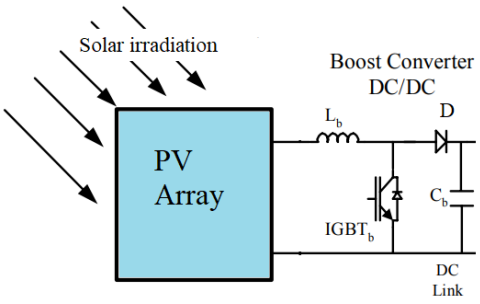

Figure 2: Solar PV plant circuit topology

The boost converter is a combination of booster inductor (L_b), IGBTb switch for voltage control, output capacitance (C_b) and blocking diode (D) [14]. The $IGBT_b$ switch is controlled by MPPT control module for maximum power extraction taking feedback from PV array voltage amplitude (V_{pv}) and current magnitude (I_{pv}). The adopted MPPT algorithm is P&O method which is considered to be traditional control with less complex structure [15]. The below figure 3 is the P&O method MPPT algorithm integrated for the control of IGBTb switch of the boost converter [16].

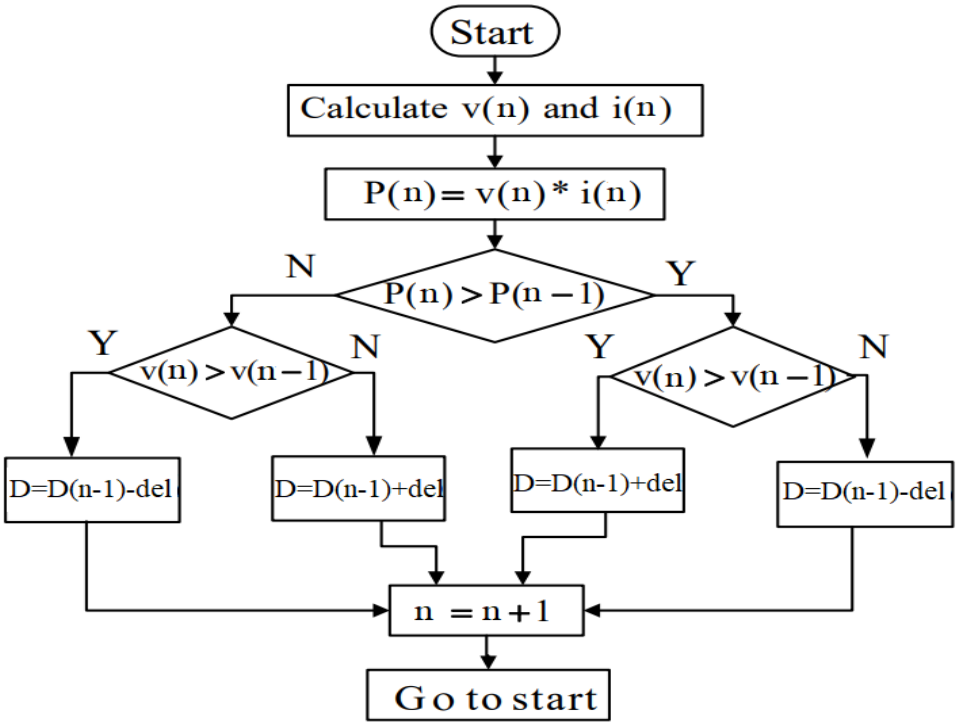

Figure 3: P&O MPPT method

As per figure 3 the present values of PV array voltage and current is denoted as v(n) and i(n) respectively. The past value of PV array voltage and power are defined by v(n-1) and P(n-1). The past power of the PV array is calculated by the expression below.

$$P(n-1) = v(n-1) * i(n-1) \quad (4)$$

Here, i(n-1) is the past value of the PV array current. With the defined variables of present and past values of PV voltage and power the duty ratio (D) of the $IGBT_b$ switch is updated as per the comparative expressions below.

$$D(n) = D(n-1) + del \begin{Bmatrix} If\ P(n) > P(n-1)\ and\ V(n) > V(n-1) \\ If\ P(n) < P(n-1) amd\ V(n) < V(n-1) \end{Bmatrix} \quad (5)$$

$$D(n) = D(n-1) - del \begin{Bmatrix} If\ P(n) < P(n-1)\ and\ V(n) > V(n-1) \\ If\ P(n) > P(n-1) amd\ V(n) < V(n-1) \end{Bmatrix} \quad (6)$$

In the above expressions D(n) is the present value of duty ratio, D(n-1) is the previous value of duty ratio and 'del' is the fraction update of duty ratio either added or subtracted with respect to the relation in (4) and (5) [17]. The updated duty ratio by the 'del' value is compared to high frequency saw-tooth waveform for generation of pulses to the $IGBT_b$ switch controlling the output of the boost converter.

B. Wind Farm

The wind farm renewable source generates power using natural source wind flow making the propeller to rotate in turn rotating the generator through turbine for power generation. There are two types of wind farms, onshore and offshore. The onshore wind farms are placed on land where the air blows from sea to land and the offshore wind farms are place in water (sea) where the air blows from land to sea. From these types the onshore wind farms are considered to be more viable and simple for installation. In this paper a PMSG (Permanent Magnet Synchronous Generator) wind generation unit is considered which is a standalone renewable source [18]. The PMSG rotor is permanent magnet, mechanically coupled to wind turbine which rotates as per the propellers rotation through a gear box.

The PMSG generates power as per the wind speed which is unpredictable to estimate. Therefore, the voltage and power output of the generator is not constant [19]. To make the voltage constant a two stage converter is adopted which includes two back to back connected voltage source converters (VSCs) names as machine side converter (MSC) and GSC (grid side conveter) . The PMSG wind farm topology is presented figure 4.

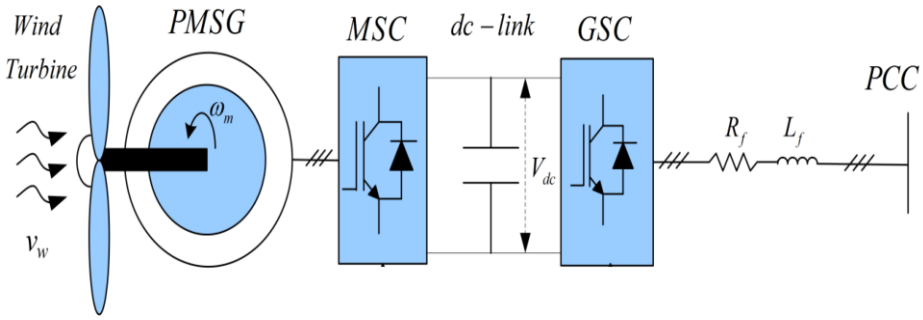

Figure 4: PMSG wind farm with two stage converters

Both the converters are controlled by Sin PWM pulses with reference signals generated by individual control structures. The MSC operates in synchronization to the PMSG electrical rotor angle (wr) and the GSC operates in synchronization with the grid electrical angle (we). The MSC converts the unregulated PMSG AC voltages to regulated DC voltage and the regulated DC voltage is converted to required AC voltages by the GSC [20]. The power from the PMSG is shared to the grid through these converters. The controller for these converters are presented in figure 5(a) and 5(b).

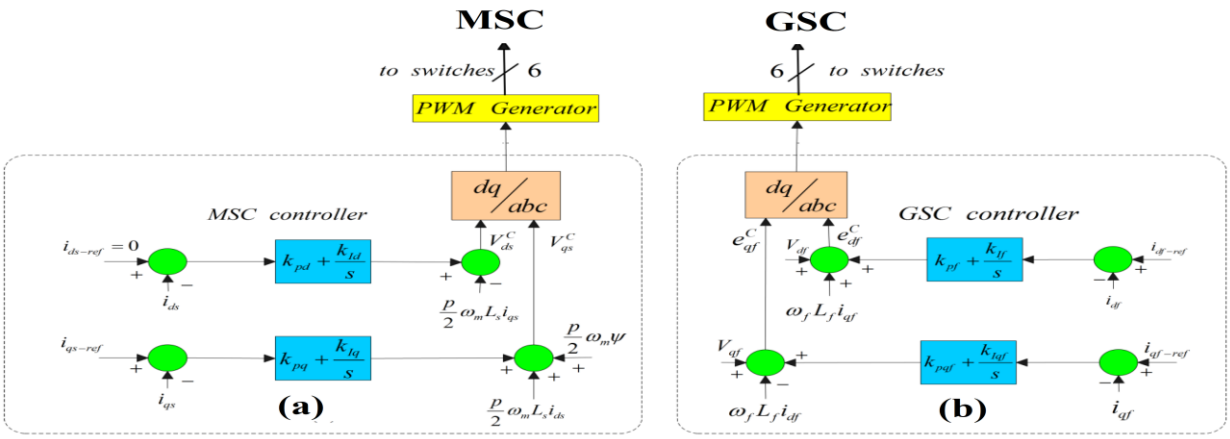

Figure 5: (a) MSC controller (b) GSC controller

The reference signals for the PWM generator are generated by the reference and measured current dq components of grid and stator. The dq current components are generated by the Park's transformations with electrical angles generated by the Phase Locked Loop (PLL) [21]. The below are the set of equations for generation of reference signals for the MSC and GSC.

$$V_{ds}^{C} = \left(\left(i_{ds-ref} - i_{ds}\right)\left(k_{pd} + \frac{k_{id}}{s}\right)\right) - \left(\frac{p}{2}\, w_m L_s i_{qs}\right) \quad (7)$$

$$V_{qs}^{C} = \left(\left(i_{qs-ref} - i_{qs}\right)\left(k_{pq} + \frac{k_{iq}}{s}\right)\right) + \left(\frac{p}{2}\, w_m L_s i_{ds}\right) + \left(\frac{p}{2}\, w_m \psi\right) \quad (8)$$

$$e_{df}^{C} = \left(\left(i_{df-ref} - i_{df}\right)\left(k_{pdf} + \frac{k_{idf}}{s}\right)\right) + \left(w_f L_f i_{qf}\right) + V_{df} \quad (9)$$

$$e_{qf}^{C} = \left(\left(i_{qf-ref} - i_{qf}\right)\left(k_{pdf} + \frac{k_{iqf}}{s}\right)\right) - \left(w_f L_f i_{df}\right) + V_{qf} \quad (10)$$

Here, i_{ds-ref} i_{qs-ref} and i_{ds} i_{qs} are the reference and measured PMSG stator currents dq components respectively. k_{pd} k_{id} and $k_{pq}k_{iq}$ are the PI controller proportional and integral gains of MSC controller. 'p' is the number of pole pairs of stator, w_m is the rotor speed, L_s is stator inductance and ψ is flux constant of PSMG. i_{df-ref} i_{qf-ref} and i_{df} i_{qf} are the reference and measured GSC dq components respectively. $k_{pdf}k_{idf}$ are the PI controller proportional and integral gains of GSC controller. w_f is the grid angular frequency, L_f is the filter inductance and V_{df} V_{qf} are the GSC voltage dq components.

A. 3-ph Inverter control

The 3-ph inverter used for the conversion of the DC voltages from the PV plant or wind farm is a 6-IGBT switch conventional topology controlled by pulse width modulation (PWM) [22]. The pulses to the inverter are generated with respect to 3-ph grid voltages making the 3-ph inverter operate in synchronization to the grid. Only with the synchronization, powers from the PV panels or wind farm can be shared to the grid with similar phase angles, frequency and voltage magnitude [23]. For this synchronization a 'synchronous reference frame' (SRF) controller is adopted for the control of the 6-IGBT switch inverter. The control schematic of the SRF controller can be observed in the figure 6 below.

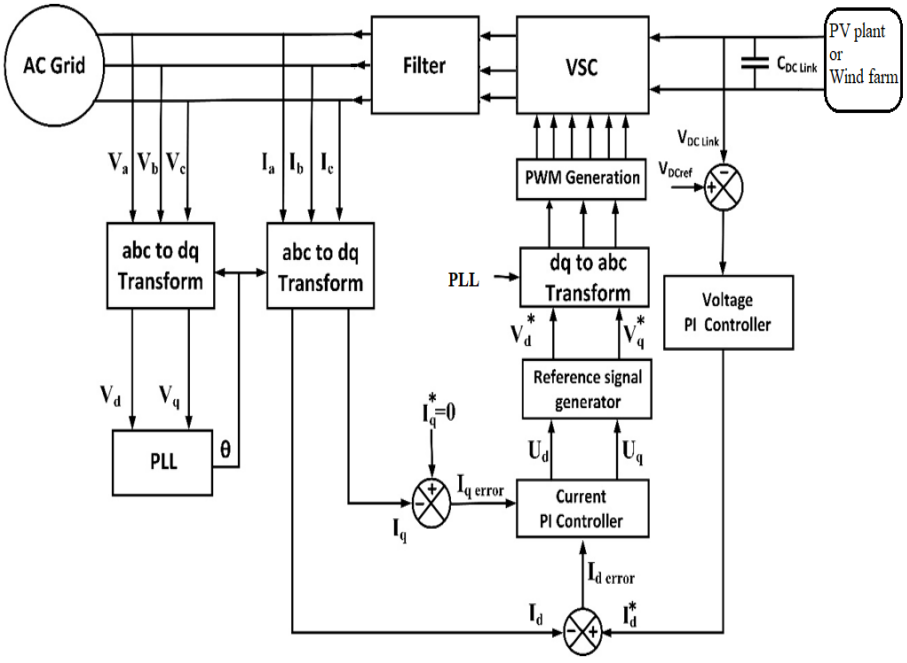

Figure 6: SRF control schematic

The reference voltages (V_{abc}*) for the PWM generation are generated by inverse Park's transformation of d-q voltage components (V_d* V_q*) [24]. These d-q components are expressed as

$$V_d^* = Ud + Vd + L\omega I_q \quad (11)$$

$$V_q^* = Uq + Vq - L\omega I_d \quad (12)$$

Here, Vd and Vq are the measured d-q components of the grid voltages, Id and Iq are the 3-ph inverter d-q currents generated by Park's transformation. From the current PI controller generating Ud and Uq the expression are given as

$$U_d = (I_d^* - I_d)(k_p + \int k_i) \quad (13)$$

$$U_q = \left(I_q^* - I_q\right)(k_p + \int k_i) \quad (14)$$

Here, Iq* is taken as '0' and the Id* is generated by the DC link voltage comparison expressed as

$$I_d^* = (V_{dc}^* - V_{dc})(k_p + \int k_i) \quad (15)$$

In every controller the kp and ki gain values are tuned as per the response of the system to the changes created in the model. They are tuned using trial and error method with less damping generated in the signals [25]. These modules are connected and renewable DG units are formed which are integrated to the IEEE 14 bus system for power sharing and performance enhancement of the system.

IV.SIMULATION ANALYSIS

The system with buses operating in the range of kV and MW is designed using the structure of IEEE 14 bus system. The modeling is done using 'Power system' tools in MATLAB simulink software generating results in graphical format. As per the data given in table 1,2 the grid is modeled with RL transmission lines representing medium range transmission lines in a grid. The below figure 7 is the modeling of the IEEE 14 bus system with all the devices connected at specific buses.

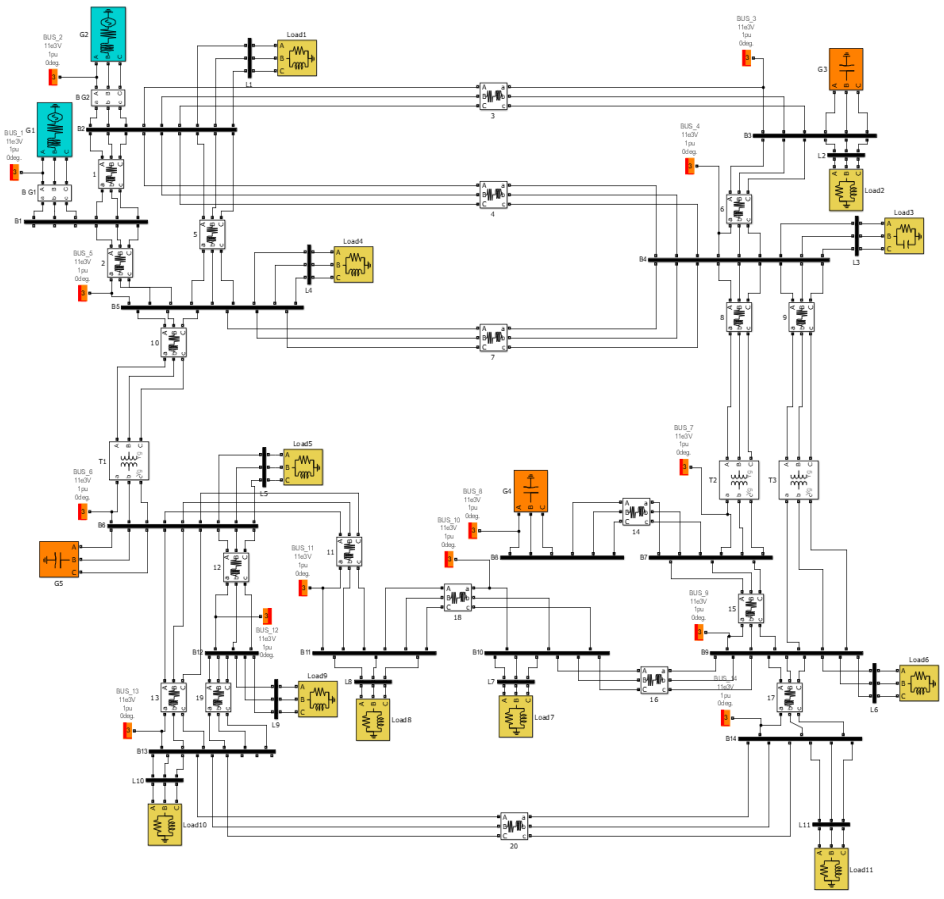

Figure 7: IEEE 14 bus system Simulink modeling

Each bus in the above bus system is connected with a load flow bus analyzer for load flow analysis of the given system using Newton-Raphson method. As per the results generated by the load flow analysis shown in table 4, the voltages are determined in per unit representation. The allowable voltage magnitudes for a healthy grid need to be maintained between 0.9 to 1.0 per unit.

With the load flow analysis the buses which have voltages below 0.9 pu are not compensated as per the demand. Due to the distance from the main sources there is loss in the lines which creates low voltages in the buses. The least two weak buses indicated are bus 13 (0.7743pu) and bus 14 (0.7884 pu). These weak buses are now updated with RGUs PV plant and wind farm for renewable power sharing.

The below are the voltages of the buses, after load flow is converged on the system using the given ratings.

Table 4: Voltages of IEEE 14 bus system

Bus No	Voltage magnitude(per unit)
1	1
2	1
3	0.9235
4	0.8961
5	0.8987
6	0.8490
7	0.8918
8	0.9204
9	0.8669
10	0.8417
11	0.7999
12	0.7947
13	0.7743
14	0.7884

The parameters of the RGUs are given in table 5.

Table 5: RGUs parameters

Name of the module	**Parameter values**
PV array	V_{mp}=54.7V, I_{mp}=5.58A, V_{oc}=64.2V, I_{sc}=5.96A, N_s=40, N_p=820, P_{pv}=10MW.
Boost converter	L_b=5mH, C_{in}=100uF, R_{diode}=0.1Ω, R_{igbt}=0.05Ω, C_{out}=12000uF.
MPPT	Del=0.05, Mppt gain=5, initial duty ratio=0.5, f_{sw}=5kHz
PMSG	575V_{dc}, 4.5rad/sec, 22.22MNm, Rs=0.027Ω, L=0.195mH, flux=0.192V.s, P=48, J=32000kg.m^2
Wind turbine	P=10MW, S_{nom}=10MW/0.9, Base wind speed=12m/s
Buck-Boost converter	Cdc=10mF, R_{igbt}=0.05Ω, R_{diode}=0.1Ω, Vdc = 1150V.
SRF controller	V_{dc}^*=500V, K_{pdc}=7, K_{idc}=800, K_{pi}=0.3, K_{ii}=20, f_{sw}= 5000Hz.

As per the given parameters two RGUs are modeled which include PV array connected to boost converter operated by P&O MPPT control and PMSG connected buck-boost converter operated by linear feedback MPPT control. Both the units are connected with 3-ph VSI operated by SRF controller with synchronization to the connected bus. The PV plant is placed at bus 14 and wind farm is placed at bus 13 of the IEEE 14 bus system. After the update to the grid the load flow analysis is carried out with the RGUs placed at two weakest buses of the system. The below is the data generated after the load flow is converged with RGUs.

As per table 6 data it is observed that the weak buses in previous analysis are improved when the system is updated with RGUs. As per the new data the bus 13 voltage is noted at 0.9340 pu and bus 14 voltage is noted at 0.9195 pu. Along with these two buses all the remaining bus voltages are also maintained above 0.9 pu which is considered to be a healthy bus system. A graphical comparison of voltage magnitudes of all the buses of the 14 bus system can be observed below with simulation time of 1sec.

Table 6: Voltages of IEEE 14 bus system after connecting RGUs

Bus No	Voltage magnitude(per unit)
1	1
2	1
3	0.9716
4	0.9653
5	0.9684
6	0.9576
7	0.9653
8	0.9805
9	0.9558
10	0.9524
11	0.9533
12	0.9427
13	0.9340
14	0.9195

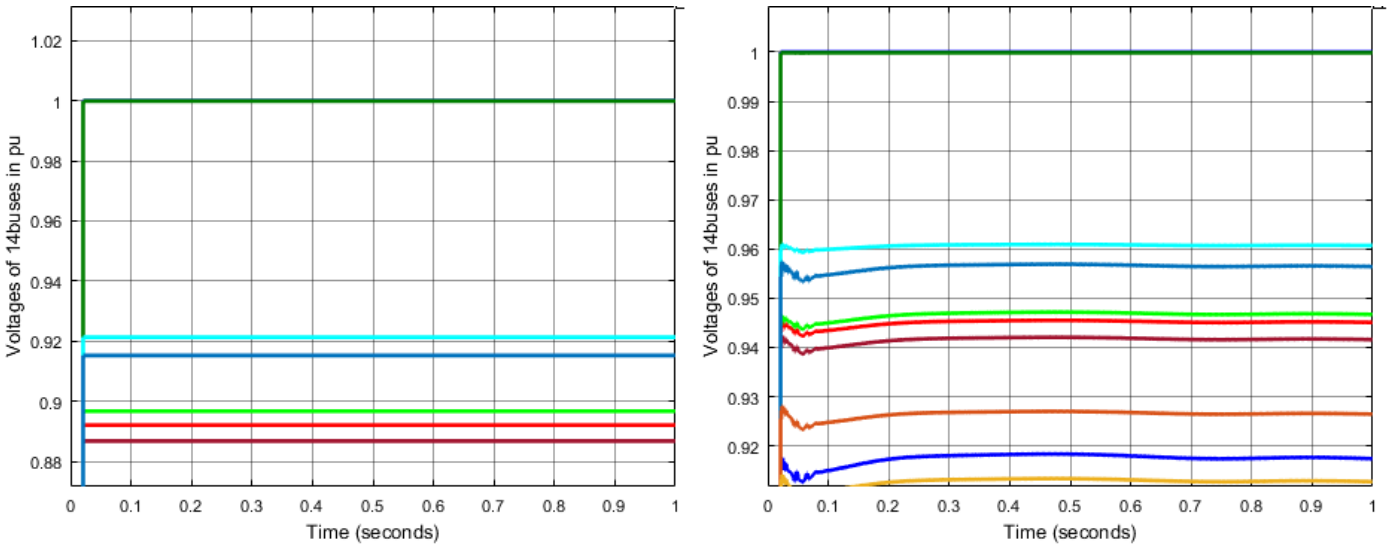

Figure 8: Voltage magnitude comparison of all buses (a) Before connecting RGUs (b) After connecting RGUs

As observed in figure 8(a) the voltages below 0.9 pu magnitude in the 14 bus system are increased above 0.9 pu magnitude in figure 8(b) when the system is integrated with RGUs. Along with voltage magnitude improvement of the buses, Power loss is reduced, Consumption of conventional source power is reduced and power factor is maintained near to unity. The below are the graphs of the parameters noted before and after connecting the RGUs.

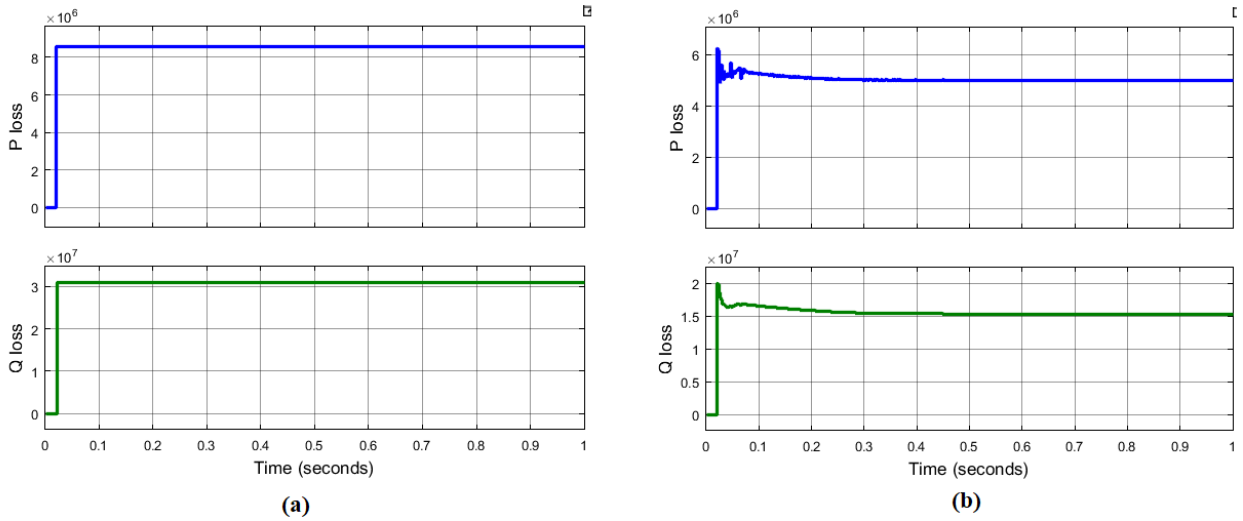

Figure 9: Power loss comparison (a) Before connecting RGUs (b) After connecting RGUs

In the figure 9(a) the power loss when the system is feeding only from the generators G1 and G2 is noted to be 8.2MW and 30MVAR. As per figure 9(b) when the 14bus MG is updated with RGUs the power loss has reduced to 5MW and 15MVAR which is half the power loss in conventional system. The comparison of the generators powers PG1 PG2 QG1 amd QG2 can be observed in figure 12 a, 12b, 13a and 13b.

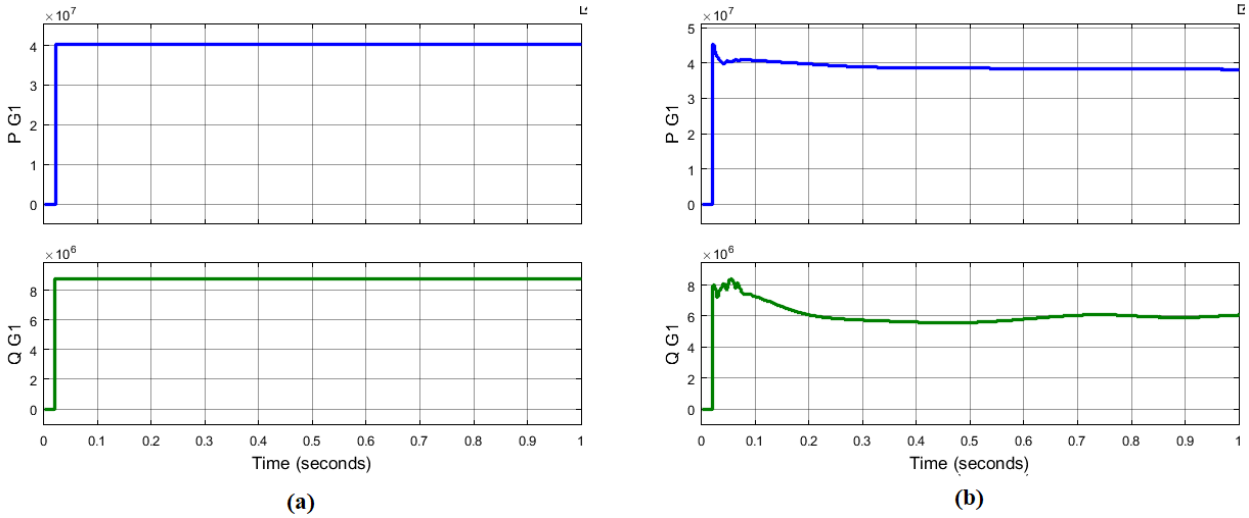

Figure 10: G1 powers comparison (a) Before connecting RGUs (b) After connecting RGUs

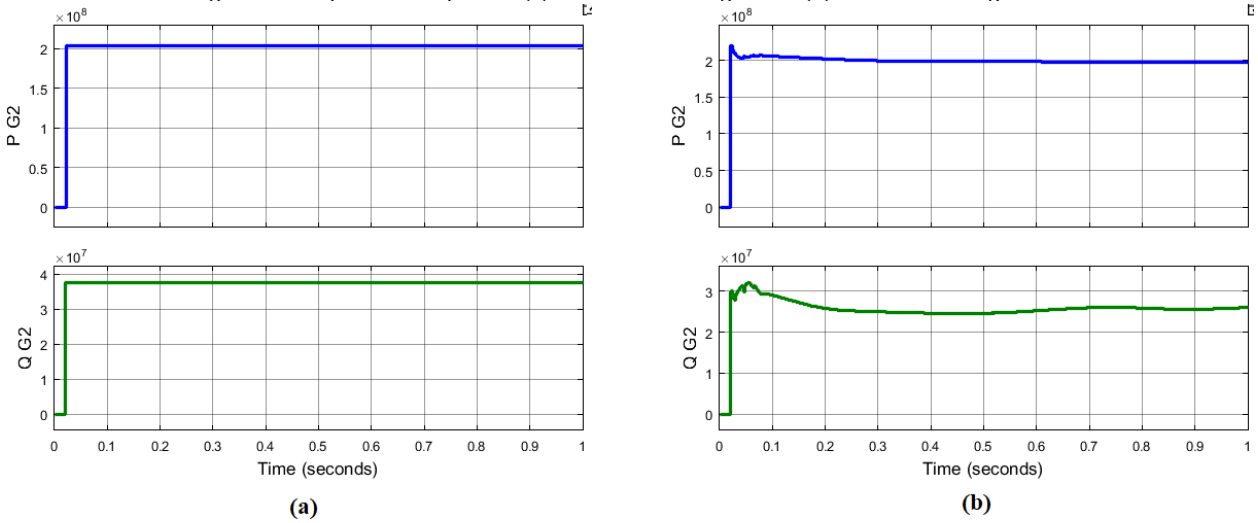

Figure 11: G2 powers comparison (a) Before connecting RGUs (b) After connecting RGUs

As observed in figure 10 and 11 there are no much changes in the power delivery from the G1 and G2 generators. The G1 delivers 40MW and and 8MVAR, G2 delivers 200MW and 35MVAR. The integration of the PV and wind farm plants reduces the losses in the system by compensating the local loads with renewable powers.

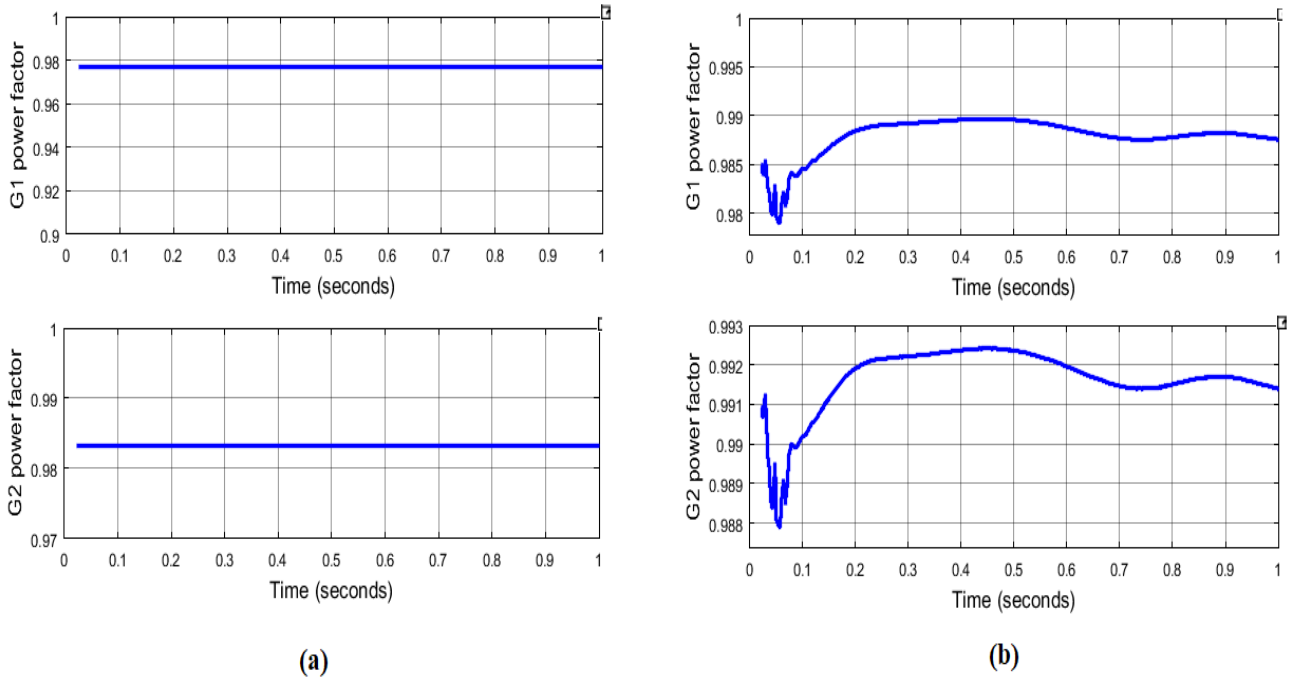

Figure 12: G1 and G2 power factors (a) Before connecting RGUs (b) After connecting RGUs

The figure 12a and 12b are the power factor comparisons of the generators G1 and G2 without and with RGUs at the weak bus locations respectively. As observed in any given condition the power factors of the generators are maintained near to unity making it an ideal bus system for power transmission. A parametric value comparison table 6 is given below validating different parameters of the system with and without RGUs.

Table 7: Parameter comparison

Name of the parameter	Without RGUs	With RGUs
Vmag at bus 13	0.7743 pu	0.9340 pu
Vmag at bus 14	0.7884 pu	0.9195 pu

V.CONCLUSION

The design and modeling of the IEEE 14 bus system is done representing a grid feeding multiple loads. Load flow analysis is done on the 14bus system using 'Newton-Raphson' method available in Simulink software to determine the voltage magnitudes.. The updated of the bus system with integration of RGUs at 13 and 14 buses improves the voltage magnitudes of all buses and also reduces power loss to half. The power consumed from the main generators G1 and G2 are maintained same with RGUs connected improving the voltage profiles of all the buses. The power factors of the generators are also maintained near to unity (0.98-0.99) in both systems without and with RGUs. Therefore with this analysis the voltage magnitudes of buses in system are determined by load flow analysis and RGUs are introduced in the system improving several parameters of the bus system.

VI.REFERENCES

[1] Ashirwad Dubey, "Load Flow Analysis of Power Systems", International Journal of Scientific & Engineering Research, vol. 7, no. 5, May 2016.

[2] S. Hou, R. Lu, C. Yang, D. Lei and W. Qin, "Power system weak bus identification based on voltage distribution characteristic," 2017 IEEE Conference on Energy Internet and Energy System Integration (EI2), Beijing, China, 2017, pp. 1-6, doi: 10.1109/EI2.2017.8245593.

[3] X. Liu and T. Zhang, "Analysis of IEEE 14 bus power flow calculation characteristics based on Newton-Raphson method," 2022 IEEE 5th International Conference on Automation, Electronics and Electrical Engineering (AUTEEE), Shenyang, China, 2022, pp. 1092-1097, doi: 10.1109/AUTEEE56487.2022.9994339.

[4] N.A M. Rosdi, A.Z. Abdullah, N. Azizan. (2022). A Simplified Analysis of Load Flow for Distribution Network Load Profile. Mathematical Statistician and Engineering Applications, 71(3), 1496–1509.

[5] D. Razmi, T. Lu, B. Papari, E. Akbari, G. Fathi and M. Ghadamyari, "An Overview on Power Quality Issues and Control Strategies for Distribution Networks With the Presence of Distributed Generation Resources," in *IEEE Access*, vol. 11, pp. 10308-10325, 2023,

[6] N.F.A. Aziz, N.A. Rahmat, F.M. Sukki, T.K.A. Rahman, Z.M. Yasin, N.A. Wahab, N.A. Salim. 2017. A New Weak Area Identification Method in Power System Based on Voltage Stability. Journal of Telecommunication, Electronic and Computer Engineering (JTEC). 9(2): 171-177

[7] Nibedita Ghosh, S. Sharma, and S. Bhattacharjee, “A load flow based approach for optimal allocation of distributed generation units in the distributed network for voltage improvement and loss minimization,” Internation Journal of Computer Applications, vol. 50, no. 15, 0975-8887, 2012.

[8] B. Poornazaryan, P. Karimyan, G.B. Gharehpetian, M. Abedi. 2016. Optimal Allocation and Sizing of DG Units Considering Voltage Stability, Losses and Load Variations. International Journal of Electrical Power and Energy Systems. 79: 42-52.

[9] Barna, Abdul & Channi, Harpreet. (2020). Load flow analysis in IEEE 14 Bus system Using FACTS Device. 29. 10617-10621

[10] S. Monemi, T. Dent and A. Nunez, "A Model of System Protection in IEEE 14-bus Power Grid," 2022 IEEE International Conference in Power Engineering Application (ICPEA), Shah Alam, Malaysia, 2022, pp. 1-5, doi: 10.1109/ICPEA53519.2022.9744697.

[11] Kheelesh Kumar Dewangan, Ashish K. Panchal, Power flow analysis using successive approximation and adomian decomposition methods with a new power flow formulation, Electric Power Systems Research, Volume 211, 2022, 108190, ISSN 0378-7796.

[12] L. Xiong et al., "Voltage and Frequency Regulation With WT-PV-BESS in Remote Weak Grids via Fixed-Time Containment Control," in IEEE Transactions on Power Systems, vol. 38, no. 3, pp. 2719-2735, May 2023, doi: 10.1109/TPWRS.2022.3190847.

[13] M. M. Gulzar, A. Iqbal, D. Sibtain and M. Khalid, "An Innovative Converterless Solar PV Control Strategy for a Grid Connected Hybrid PV/Wind/Fuel-Cell System Coupled With Battery Energy Storage," in IEEE Access, vol. 11, pp. 23245-23259, 2023, doi: 10.1109/ACCESS.2023.3252891.

[14] M. A. Awal and I. Husain, "Unified Virtual Oscillator Control for Grid-Forming and Grid-Following Converters," in IEEE Journal of Emerging and Selected Topics in Power Electronics, vol. 9, no. 4, pp. 4573-4586, Aug. 2021, doi: 10.1109/JESTPE.2020.3025748.

[15] A.F.M. Nor, M. Sulaiman, A.F.A. Kadir, R. Omar. Voltage Stability Analysis of Load Buses in Electric Power System Using Adaptive Neuro-Fuzzy Inference System (ANFIS) And Probabilistic Neural Network (PNN). 2017. ARPN Journal of Engineering and Applied Sciences. 12(5): 1406-1412.

[16] S. You et al., "Impact of High PV Penetration on Regional Power Grids," 2022 7th IEEE Workshop on the Electronic Grid (eGRID), Auckland, New Zealand, 2022, pp. 1-5, doi: 10.1109/eGRID57376.2022.9990023.

[17] S. Diao, X. Li, X. Cao, J. Li, P. Du and J. Zhuang, "Research on Operation Characteristics of Distributed PV based on Measured Data," 2021 IEEE International Conference on Predictive Control of Electrical Drives and Power Electronics (PRECEDE), Jinan, China, 2021, pp. 885-890, doi: 10.1109/PRECEDE51386.2021.9680899.

[18] L. F. Ochoa and G. P. Harrison, “Minimizing energy losses: Optimal accommodation and smart operation of renewable distributed generation,” IEEE Trans. Power Systems, vol. 26, no. 1, pp. 198–205, 2011

[19] Ulutaş, Alper & Duru, Tarık. (2019). Variable-Speed Direct-Drive Permanent Magnet Synchronous Generator Wind Turbine Modeling and Simulation. Kocaeli Journal of Science and Engineering. 2. 21-27. 10.34088/kojose.515467.

[20] Nasiri, M.; Mobayen, S.; Faridpak, B.; Fekih, A.; Chang, A. Small-Signal Modeling of PMSG-Based Wind Turbine for Low Voltage Ride-Through and Artificial Intelligent Studies. *Energies* **2020**, *13*, 6685. https://doi.org/10.3390/en13246685

[21] Y. Wang, C. Zhao, C. Guo and A. U. Rehman, "Dynamics and small signal stability analysis of PMSG-based wind farm with an MMC-HVDC system," in CSEE Journal of Power and Energy Systems, vol. 6, no. 1, pp. 226-235, March 2020, doi: 10.17775/CSEEJPES.2019.02550.

[22] A. kumar, R. Garg and P. Mahajan, "Performance Analysis of Grid Integrated PV System using SRF and IRPT Control," 2019 1st International Conference on Signal Processing, VLSI and Communication Engineering (ICSPVCE), Delhi, India, 2019, pp. 1-7, doi: 10.1109/ICSPVCE46182.2019.9092869.

[23] A. kumar, R. Garg and P. Mahajan, "Performance Analysis of Grid Integrated PV System using SRF and IRPT Control," 2019 1st International Conference on Signal Processing, VLSI and Communication Engineering (ICSPVCE), Delhi, India, 2019, pp. 1-7, doi: 10.1109/ICSPVCE46182.2019.9092869.

[24] G. E. Mejia-Ruiz, J. M. R. Guerrero, M. R. A. Paternina, J. de la Cruz, A. Zamora-Mendez and A. P. P. Sandoval, "Enhancing Grid Integration and Design of Low Speed PMSGs by Exploiting SRF-PLL-Based Sensorless Control and Holistic Modeling," in IEEE Transactions on Energy Conversion, vol. 37, no. 4, pp. 2962-2973, Dec. 2022, doi: 10.1109/TEC.2022.3199166.

[25] M.Pushpanjalli, Dr.M.S.Sujatha, “A Navel multi objective under frequency load shedding in a micro grid using genetic algorithem”, International journal of Advanced Research in Electrical, Electronics and Instrumentation Engineering, ISSN:2278-8875, Vol:4, Issue:6, June,2015.

BIOGRAPHIES OF AUTHORS

Boya Harika is research scholar at Electrical Engineering Department University College of Engineering, Osmania University. Her research areas are power system and power quality. She can be contacted at email: harikagnits@gmail.com.

Dr. Bhaskaruni Suresh Kumar is Associate Professor at Electrical and Electronics Engineering Department *in* Chaitanya Bharathi Institute of Technology, Osmania University. He holds a PhD degree in Power Quality-Power Systems in the year 2014 from JNTU Kukatpally, Hyderabad, Telangana. His research areas are power system, and power quality. He can be contacted at email: bskbus@gmail.com.

Dr. Jalla Upendar is Assistant Professor at Electrical Engineering Department University College of Engineering, Osmania University. He holds a PhD degree in Intelligent Approach for Fault Classification of Power Transmission Systems with specialization in Electrical Engineering in Indian Institute of Technology (IIT), Roorkee, Uttarakhand, India in 2010. His research areas are power system, power electronics, FACTS devices, and artificial intelligent techniques. He can be contacted at email: dr.8500003210@gmail.com.